Proceedings of the Sixth International Conference on
Railway Technology: Research, Development and Maintenance
Edited by: J. Pombo
Civil-Comp Conferences, Volume 7, Paper 8.15
Civil-Comp Press, Edinburgh, United Kingdom, 2024
ISSN: 2753-3239, doi: 10.4203/ccc.7.8.15

Demonstration of smart autonomous AI ultrasonic inspections to TRL 7

I. Durazo-Cardenas

**School of Aerospace, Transportation and Manufacturing
Cranfield University
Cranfield, United Kingdom**

Abstract

This research successfully demonstrated the feasibility of autonomous ultrasonic rail inspections up to technology readiness level (TRL) 7. A prototype integrating an autonomous rail vehicle and the latest artificial intelligence (AI) Sperry's ultrasound testing (UT) system was used for these demonstrations. The project initially demonstrated TRL5 attainment at Cranfield's Railways Innovation Test Area (RITA). It was then prepared for a series of tests at a heritage operational railway to achieve TRL 7 attainment. Experimental works included nine rounds of tests on a 250-meter track inspection, showcasing inspection, localization, navigation accuracy, and defect location precision. The prototype successfully detected all the simulated rail defects and reported to the command centre as required. The vehicle performance was characterised by measuring its positional error and detection rate. The verified odometry and GPS positional measurements revealed errors ranging from 0.27 to 3.2 m and up to 8 m, respectively. The absence of differential GPS and an unrefined fusion approach contributing to these errors. Weak 4G signal coverage during field tests impacted operator-vehicle communication and data uploading rates. Future iterations should address these limitations, exploring alternatives for enhanced accuracy and advancing defect-sizing technology.

Keywords: smart railway maintenance, autonomous, artificial intelligence, maintenance automation, automated railway systems, smart operation and maintenance

1 Introduction

The railways are an essential transportation system. Increasing demands put considerable pressure on the existing infrastructure, including tracks. As a result, the railways infrastructure maintainers face significant challenges in improving the network availability, and reliability. Smart systems are considered an essential step forward [1].

Typical ultrasonic inspections involve a specialist ultrasonic testing unit (UTU) performing an initial survey which identifies fault suspects. These are followed by on-foot ultrasonics inspector that first scans, locate, size and confirms the fault before a repair is enacted.

However, labour-intensive operations significantly raise safety risk concerns and inspection costs. UK's Rail staff suffered 83 specified injuries on all rail networks from 2022 to 2023 [2]. Safety concerns are one of the main change drivers in developing new autonomous inspection and repair systems alongside a need for consistent mechanistic interpretation of results, cost effectively [3], [4].
Recent academia and industry collaborations developed autonomous rail inspection systems to reduce pedestrian inspections, which can mitigate the above issues. For example, Liu et al. [5] reported the development of an autonomous rail-road amphibious robotic prototype for railway inspection and maintenance tasks. It comprised a trolley platform, and an off-the-shelf all terrain unmanned ground vehicle equipped with a robotic manipulator. Rahman et al. [6] analysed the dynamic principles of the system and proposed a health assessment based on 3D reconstruction technology for railway track maintenance by combining multiple sensing and taking advantage of the robotic manipulator camera [7]. The developed system was demonstrated in both operational and realistic track environments with multiple testing activities ranging from remote operation, navigation, accurate job detection, inspection, and repair, job completion communication and human supervision/interaction [5]. Furthermore, Durazo-Cardenas et al. integrated a commercially available ultrasonic instrument to the system and demonstrated the autonomous ultrasonic rail inspection to Technology Readiness Level 5 [8], [9]. While these previous attempts proved the command-and-control architecture functionality, the test vehicle exhibited poor dynamic performance, and it was found cyber-vulnerable.

Following on from these recent studies, the present research aims to advance the demonstrated autonomous ultrasonic inspection functionality to a higher TRL. The works encompassed the development and demonstration of a new autonomous inspection prototype with the integration of a commercial ultrasonic inspection unit in an operational environment. It is worth noting that this project does not involve the development of new inspection technology. Instead, it deployed the latest available Artificial Intelligence (AI) cloud-based ultrasonic rail inspection solution with the latest autonomous rail vehicle research advancements.

2 Methods

This research discarded the original prototype developed by Liu. et al [5]due to its poor dynamic performance and cybersecurity vulnerabilities introduced by the Robot Operation System (ROS) 1 framework. A new generation prototype was then developed with the integration of an autonomous rail flatbed vehicle and an ultrasound testing system from Sperry®.

The new autonomous rail vehicle used was built upon a manual-controlled motorised trolley from BANCE®. It was procured and upgraded to become an autonomous robot platform capable of self-navigation and obstacle avoidance functionality using a more secure ROS 2 framework [10], see Figure 1. This vehicle is lightweight, battery-powered, and capable of carrying a payload of up to 830 kg while reaching speeds of up to 8 km/h. In order to implement autonomous a more straightforward driving capability, seven speed levels were pre-defined covering the vehicle speed range.

Figure 1 Autonomous Rail Trolley, equipped with LiDAR, GPS, Encoder and Camera

2.1. Ultrasonic Inspection System

A commercial ultrasonic rail inspection system from Sperry® Rail Inc. was integrated with the new autonomous rail vehicle. The inspection system comprises Sperr's proprietary Ultrasonic 9 Probe Array (UX9) Roller Search Units (RSUs), rugged computer for data acquisition and control centre, modem, batteries, and a water tank. This inspection equipment can record the echo signals with corresponding GPS and odometry tags. Sperry's cloud AI rail flaw detection system, Elmer®, provides the software support to process the data collected by RSUs and then returns the diagnosis information to the inspector.

2.2 System integration

Given that the autonomous vehicle and UT system are two distinct systems that were not originally part of the same system, mechanical and communication interfaces were necessary to facilitate their seamless operation.

The inspection system and trolley platform are joined by simply using an aluminium fixture. The computer, batteries and water tank were positioned at the vehicle front platform and secured in place with foam energy absorbers to suppress vibrations. Since the inspection system does not inherently possess an autonomous inspection capability, the researchers established a serial port communication interface protocol between the vehicle and UT system to enable control of the inspection procedure and start and stop functions. Three string commands were employed. Initially, UT system transmitted the 'CTR_RD' command to the vehicle to indicate that inspection kit is on standby. Subsequently, the vehicle sends the 'CTR_ST' command to the UT system to initiate the inspection process, while the 'CTR_SP' command is used to terminate data collection. The integrated prototype is shown in Figure 2.

Fig.2 Integrated autonomous ultrasonic rail inspection system prototype.

2.3. Experimental Demonstration

The inspection demonstration was conducted on a heritage railway situated at Idridgehay, Derbyshire, UK. This site was used because of pre-existing calibration rails and test track containing multiple simulated defects trusted for calibration purposes by Network Rail. These calibration rails span a total length of approximately 15 meters. Table 1 lists the information about the artificial defects present in the three rails. The inspection results can be analysed by making a comparison with this data.

2.1. Inspection test procedure

Approximately 250 metres of the test track was used for the demonstration tests. The prototype departure position was established approximately 150 meters before the rails with simulated defects, while the end point of the test was 250 meters further away. This end point location was selected because in previous tests it showed strong signal coverage, which we expected would facilitate the test data upload to the cloud analyser.

Rail No.	Defect location	Defect Type	No. of Defects	Specifications
1	Rail End	Inclined flat bottom hole	2	
1	Rail Head	Through Hole	4	Φ6, 500mm interval
2	Rail End	Inclined flat bottom hole	1	
2	Rail foot (Lower Surface)	Slot	2	Two slots of 5mm depths with 500mm interval
2	Rail End's head	Flat bottom hole	4	Φ5, 100mm depth

Table 1 Defects summary for the calibration test rails.

Several traffic cones were positioned alongside the tracks allowed the researchers to visually identify specific test locations and protype actions. The precise distances separating the cones are listed in Table 2.

Cone	Distance from the base (m)	Representation
Yellow	97.1	Approaching phase endpoint
Red	146.15	Starting point for inspection
Blue	172	Endpoint for flawed rails
White marker near the track	253.9	Endpoint for test

Table 2 Specific locations and corresponding traffic cones

2.2. Tests sequence

Figure 3 depicts the vehicle speed profile during the demonstration. It illustrates the communication commands between the vehicle and the inspection system. Each test run comprises four steps: approach, inspection, and data transmission, and return to base. The inspection speed was set higher than the approaching speed because the ultrasonics (UT) system requires a minimum data collection speed of 5 km/h to avoid false positives related the fishplate joints identified as defects.

Figure 4 details the corresponding sequence flow chart. The UT system issued a ‘CTR_RD’ command to the vehicle when the prototype was positioned at the base and remained in a standby state. The operator then initiated the sequence command to commence the procedures. During Stage 1, the approaching phase, the vehicle proceeded from the base to the yellow cone position at speed level 4 until it reached the yellow cone, where it stopped momentarily before resuming acceleration to reach speed level 6 prior to the red cone. At this point, the vehicle transmitted the “CTR_ST” command to the UT system to initiate data collection at the red cone location. The prototype then continued to propel the probes at speed level 6 until it reached the blue cone and issued the “CTR_SP” command to cease inspection work. Subsequently, the vehicle reduced its speed to level 4, arriving at the data uploading point, which marks the endpoint of the test. The prototype remained in this location for a duration of 2 minutes to enable the uploading of the acquired data. Finally, the prototype navigated to the base at a speed level 4 and remained in standby mode, awaiting further instructions.

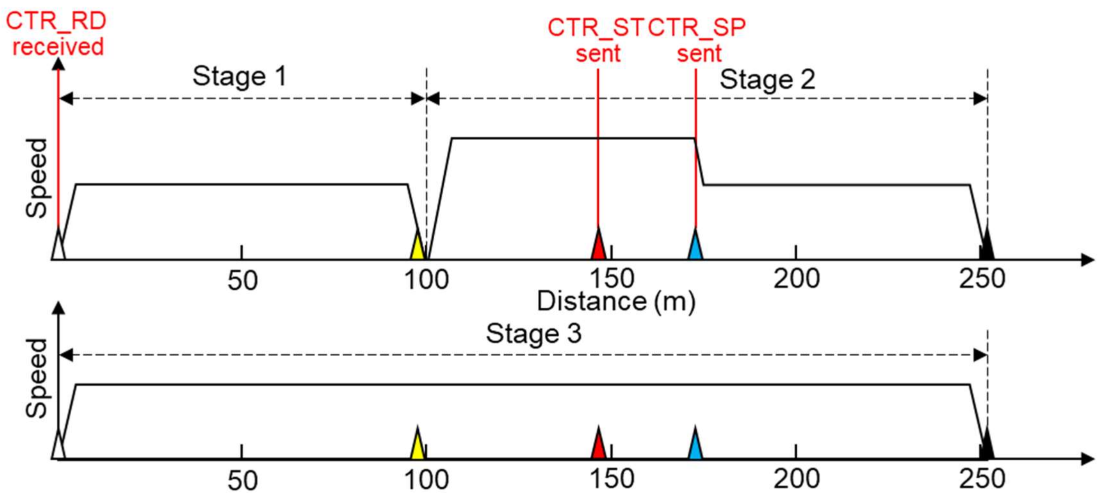

Figure 3 Speed diagram of the demonstration. The horizontal coordinate represents the distance of the prototype from the departure point.

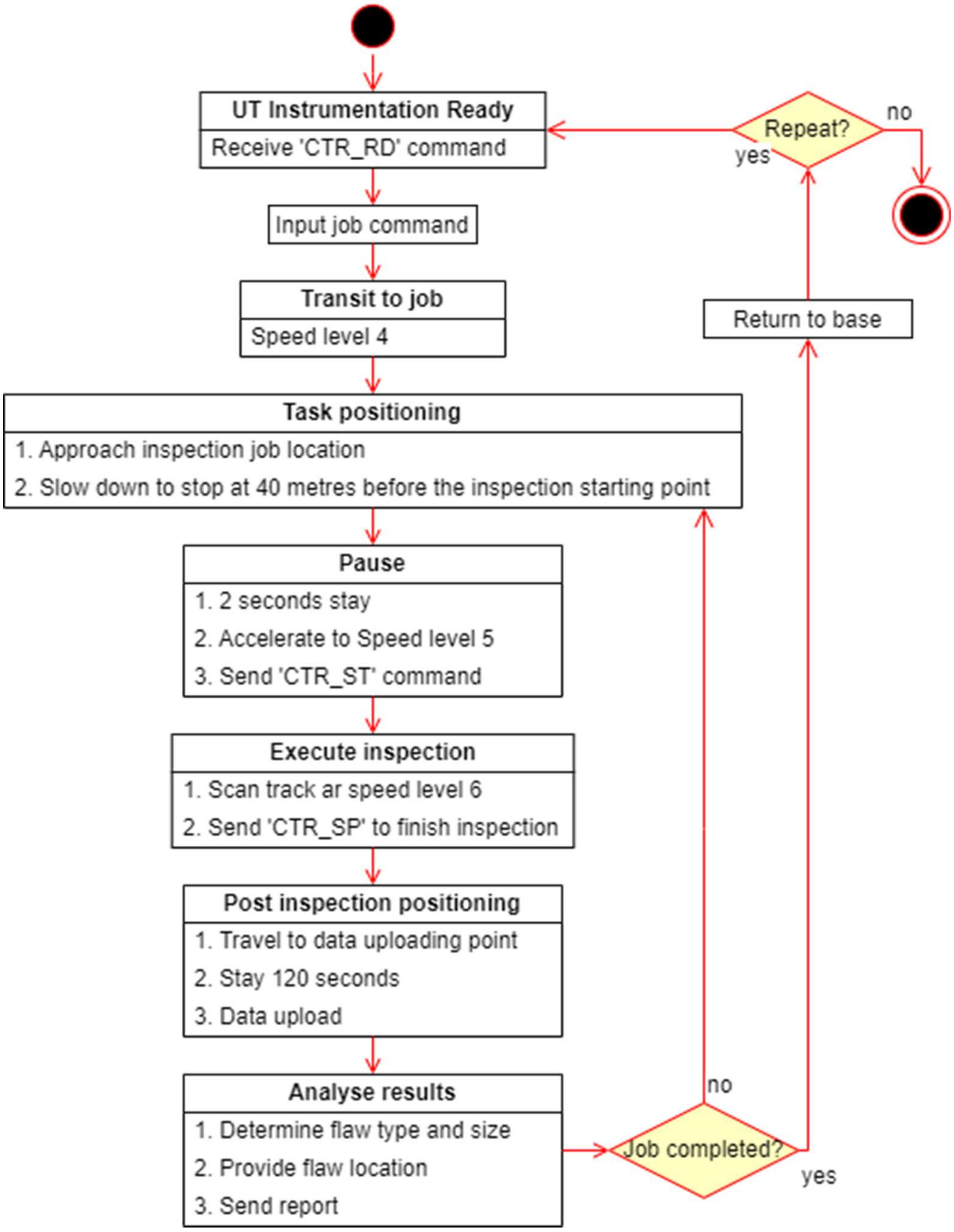

Fig.4 Flow chart of the sequence in the demonstration

3 Results

The inspection test was repeated nine times. Each time the prototype executed the required navigation successfully. The repetitive trials substantiated the feasibility and practicality of the autonomous rail inspection system. Nonetheless, during the first seven rounds of testing, the data upload phase failed because of the weak communication signals, preventing UT system from establishing a connection to the network. To enable for the date interpretation, a mobile hotspot was employed to provide mobile network access. experiments. As a result, in the eighth trial, the data was uploaded manually to the cloud-based analyser, while in the last iteration, the data was uploaded automatically upon the prototype's arrival at the designated data uploading location.

3.1. Navigation accuracy investigation

Prior tests of the GPS system localisation system accuracy were conducted at the outdoors laboratory at Cranfield University. During the tests the prototype was stationary. It was observed that the GPS system detected a total of 20 satellites, of which 19 were used for localisation during this measurement. Table 3 shows the actual and measured latitude/longitude coordinates with the error.

	Actual GPS sensor location	Measured GPS sensor location	Error (m)
Latitude	52.066605	52.066610	1.91
Longitude	-0.626347	-0.626324	

Table 3 GPS observed errors prior to test.

The localisation error was found to be approximately 1.91 metres. This was considered a relatively poor performance. Unfortunately, the GPS accuracy exhibited even a worse performance at heritage railway test site. Initial coordinates offset errors started at approximately 15 metres and gradually improved to roughly 8 metres before stabilising at this level. Therefore, it is recommended to implement differential GPS combined with odometry to improve the localisation performance to a more accurate level.

The overall positional error was measured upon return of the vehicle to base. Each return it came to a stop at a slightly different position from its initial starting point. The corresponding error was measured and analysed, see Table 4 and Figure 5. Eleven datapoints were collected from the initial rehearsals and tests. The positive and negative values indicated that the prototype either stopped before or surpassed the starting point, respectively. Notably, the error distribution appeared to be relatively arbitrary, spanning from -1.45 to 3.2 meters. The average error was approximately 0.29 meters. However, when accounting for the absolute value of the error, the mean value increased to 1.1 meters. The source of the observed odometry error was determined to be wheel slippage during the trolley operation.

	Test No.	Error (m)	Absolute error (m)
Rehearsal	1	3.2	3.2
	2	1.7	1.7
Test	1	-0.85	0.85
	2	-0.5	0.5
	3	-1.45	1.45
	4	1	1
	5	-0.27	0.27
	6	-0.52	0.52
	7	-0.84	0.84
	8	1.05	1.05
	9	0.72	0.72
Mean		0.29	1.1

Table 4 Positional error summary

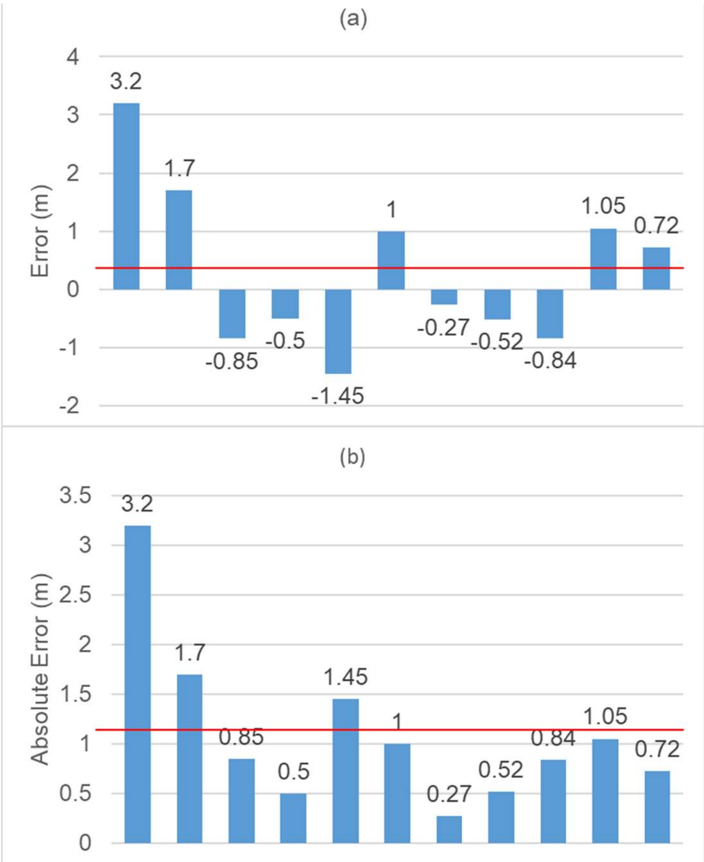

Figure 5 Measured Error of each test (Red line represents the mean value)

3.2. Inspection results investigation

The data collected from the final test iteration was successfully uploaded to Elmer®. This dataset was subsequently employed to identify rail defects. The defect size was estimated, the defect type was classified, and a final defect list comprising the defect type, size, and location information was automatically generated. Following data processing, the suspect list was automatically forwarded to a designated email address.

Upon completion of the sorting process, the defect information has been organized and part of them are presented in Table 5. The term 'measured intervals' refers to the distance between a given defect and the preceding defect that was detected.

Detected Defect No.	Artificial defects	Suspect type	Odometry distance to the first suspect (m)	Measured intervals from Odometry (m)	GPS Distance to the first suspect (m)	Measured intervals from GPS (m)
1		70Cluster	0	0	0.00	0.00
2		Bolt Hole Crack (BHC)	0	0	0.09	0.09
3		Transverse Defect (TD)	0	0	0.20	0.11
4	Through hole	70Cluster	0.8	0.8	1.88	1.67
5	Through hole	70Cluster	1.28	0.48	1.88	0.00
6	Through hole	TdSmall	1.76	0.48	1.88	0.00
7		TD	1.76	0	1.88	0.00
8	Through hole	70Cluster	2.24	0.48	1.88	0.00
9		70Cluster	5.12	2.88	5.45	3.57
10		TdSmall	5.12	0	5.52	0.07
11		BHC	10.88	5.76	11.52	6.00
12		BHC	14.24	3.36	14.75	3.23
13		BHC	14.72	0.48	15.09	0.33

Table 5 Detected defect list for the right rail

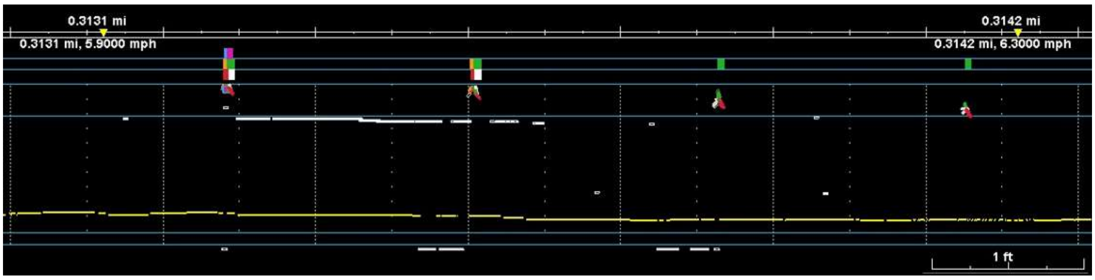

Fig.6 B-Scan images for the through-hole defects at the rail head of the right rail. Different colour marks represent the correct trigger of probes at different angles.

A total of 28 defects were detected on the track, with 13 of these present on the right rail and the remaining 15 on the left rail. Comparing the detected and actual defects, we could detect all through holes in both the left and right rails successfully. For instance, Figure 6 presents a B-Scan image captured during the inspection, highlighting the UT system's successful detection of through-hole defects on the rail head of the right rail.

On occasions, the system may classify a single defect occurring as distinct categories, denoting them, for instance, as No. 6 and No. 7 defects in the right rail. Regrettably, due to the limited available data, the research was unable to establishing a correlation between the other potential suspects and the actual defects.

As for the defect localisation, it becomes apparent that there is a lack of consistency between the odometry and GPS data with respect to the location of each individual defect. Our level of confidence in the odometry data exceeds that of the GPS data, primarily because the GPS sensors of the UT system were placed on the vehicle, providing a relatively accurate approximation of its position rather than that of the probes. Moreover, it is important to note that the GPS data was derived from the nearest available latitude and longitude coordinates, thus introducing a certain degree of measurement uncertainty.

With regards to the positioning derived from the odometry data, as illustrated in Table 5, it can be observed that the measured intervals between Defect No.4 and Defect No.8 remain consistent at 0.48m. This value is almost identical to the actual intervals of 0.5m. This outcome serves to confirm the accuracy of the UT system's odometry-based positioning methodology.

4 Conclusions and Contributions

The presented research aimed to demonstrate the feasibility of autonomous rail inspection at TRL 7, which was successfully achieved. An autonomous ultrasonic rail inspection prototype was developed by integrating an autonomous rail vehicle and a commercial UT system. Mechanical, electrical and communications integration between the vehicle and the UT system were achieved both physically and architecturally. The assembled prototype was tested its inspection capabilities at the calibration track at an operating heritage railway at operational environment, complying with TRL 7. The system's performance, including the vehicle's localization and navigation accuracy, inspection capacity, and defect location accuracy, was investigated during the demonstration. The following conclusions can be drawn:

- Autonomous rail inspection functionality has been demonstrated up to TRL 7.
- A novel autonomous rail inspection system was developed, utilizing a commercial UT system and an autonomous rail vehicle. The protype was carefully calibrated and rigorously tested.
- During a demonstration on the heritage track, the prototype successfully detected artificial rail defects, generating a downloadable suspect list that was promptly communicated to the operator via email.
- The prototype's positioning accuracy was thoroughly investigated using GPS and odometry techniques. The odometry-based positional error was found to range between 0.27 and 3.2 metres, while the largest error, around 8 metres, was associated with GPS measurements.

The following rectifiable limitations were found:

- The prototype's localization accuracy was limited by the absence of differential GPS, which resulted in large errors in the GPS positioning. To improve positioning performance, a potential solution is to apply differential GPS, install encoders on trailing wheels, and fuse data from IMU, GPS, and odometry sensors. Alternative solutions include track-side object detection relative to LiDAR and ballast pattern recognition.
- The prototype demonstrated the capability to provide an initial estimation of the defect size, although it cannot provide an exact measurement yet. The development of automatic defect sizing capability is still required with the utilisation of more advanced algorithms, more extensive datasets and test procedures to enhance accuracy and precision.
- Communication signal strength was found to be extremely weak, thereby adversely affecting both the operator-vehicle communication and data-uploading procedure of the Sperry system.

Acknowledgements

This project has received funding from the Shift2Rail Joint Undertaking (JU) under grant agreement No 826255. The JU receives support from the European Union's Horizon 2020 research and innovation programme and the Shift2Rail JU members other than the Union.

References

[1] “IN2SMART2.” Accessed: Jun. 07, 2024. [Online]. Available: https://projects.shift2rail.org/s2r_ip3_n.aspx?p=IN2SMART2
[2] O. of Rail, “Rail Safety April 2022 to March 2023”.

[3] M. Taylor, M. Westwood, and A. Peters, “A modular approach to automation of condition monitoring and repair for rail,” *IET Conference Publications*, vol. 2016, no. CP701, 2016, doi: 10.1049/CP.2016.1198.
[4] Office for road and rail, “Annual efficiency and finance assessment of Network Rail 2023”.
[5] H. Liu *et al.*, “An autonomous rail-road amphibious robotic system for railway maintenance using sensor fusion and mobile manipulator,” *Computers and Electrical Engineering*, vol. 110, p. 108874, Sep. 2023, doi: 10.1016/J.COMPELECENG.2023.108874.
[6] M. Rahman, H. Liu, I. D. Cardenas, A. Starr, A. Hall, and R. Anderson, “Towards an Autonomous RIRS: Design, Structure Investigation and Framework,” *2021 7th International Conference on Mechatronics and Robotics Engineering, ICMRE 2021*, pp. 164–168, Feb. 2021, doi: 10.1109/ICMRE51691.2021.9384846.
[7] M. Rahman, H. Liu, M. Masri, I. Durazo-Cardenas, and A. Starr, “A railway track reconstruction method using robotic vision on a mobile manipulator,” *Comput Ind*, vol. 148, Jun. 2023, doi: 10.1016/J.COMPIND.2023.103900.
[8] I. Durazo-Cardenas, A. Starr, W. Nofal, H. Liu, M. Rahimi, F. He, M. Poulter, "Demonstration of an autonomous ultrasonic testing concept for rail flaws inspection", in J. Pombo, (Editor), "Proceedings of the Fifth International Conference on Railway Technology: Research, Development and Maintenance", Civil-Comp Press, Edinburgh, UK, Online volume: CCC 1, Paper 10.23, 2022, doi:10.4203/ccc.1.10.23
[9] F. He *et al.*, “A practical demonstration of autonomous ultrasonic testing for rail flaws inspection”.
[10] J. Li, I. Durazo-Cardenas, C. Ruiz-Carcel, and A. Starr, “Smart railways: the design and construction of an autonomous inspection and maintenance vehicle” in *34th CIRP Conference*, Cranfield, May 2024.